International Journal for Parasitology 56 (2026) 104757

Contents lists available at ScienceDirect

International Journal for Parasitology

journal homepage: www.elsevier.com/locate/ijpara

Callunene, mitophagy, and flagellum removal in trypanosomatids

Andreu Saura [a,1], Vilém Blahout [b,1], Edubiel A. Alpizar-Sosa [a], Haoshen Wen [a], Aditya Reddy [a], Galina Prokopchuk [c,d], Julius Lukeš [c,d], Tereza Kubátová [b], Wim Dehaen [b,e], Silvie Rimpelová [f], Alexei Yu. Kostygov [a,g], Pavla Perlíková [b,h,*], Vyacheslav Yurchenko [a,*]

[a] Life Science Research Centre, Faculty of Science, University of Ostrava 710 00 Ostrava, Czechia
[b] Department of Organic Chemistry, Faculty of Chemical Technology, University of Chemistry and Technology, 166 28 Prague, Czechia
[c] Institute of Parasitology, Biology Centre, Czech Academy of Sciences, 370 05 České Budějovice, Czechia
[d] Faculty of Science, University of South Bohemia, 370 05 České Budějovice, Czechia
[e] Department of Informatics and Chemistry, Faculty of Chemical Technology, University of Chemistry and Technology Prague 166 28 Prague, Czechia
[f] Department of Biochemistry and Microbiology, Faculty of Food and Biochemical Technology, University of Chemistry and Technology Prague 166 28 Prague, Czechia
[g] Zoological Institute of Russian Academy of Sciences, 199034 St. Petersburg, Russia
[h] Institute of Organic Chemistry and Biochemistry, Czech Academy of Sciences, 160 00 Prague, Czechia

ARTICLE INFO

Article history:
Received 8 September 2025
Received in revised form 4 December 2025
Accepted 6 December 2025
Available online 9 December 2025

Keywords:
Callunene
rlagellum removal
Crithidia bombi
mitophagy

ABSTRACT

Callunene, a natural component of heather (*Calluna vulgaris*) nectar, has previously been shown to protect bumblebees from infection by the trypanosomatid *Crithidia bombi*. Here, we demonstrate that callunene exhibits antiparasitic activity against several trypanosomatid species, including *Crithidia bombi*, *Leishmania mexicana*, and *Trypanosoma brucei*. Notably, callunene's in vitro efficacy against *T. brucei* was comparable to that of nifurtimox, although its cytotoxicity toward human cells may limit direct therapeutic application. Using a biotinylated callunene analog in the pull-down assay, we identified NIPSNAP, a mitochondrial protein involved in mitophagy regulation, as a primary molecular target of this compound in *C. bombi*. Moreover, callunene alters acidocalcisome abundance, further connecting its role to regulation of mitochondrial physiology. Given its effects on mitochondria and ability to interact with NIPSNAP, callunene represents a promising chemical probe for studying mitophagy, a poorly understood process in trypanosomatids, and may provide new insights into mitochondrial biology of these parasites.

1. Introduction

Trypanosomatids is a group of parasitic protists that include causative agents for a number of serious human and animal diseases, such as leishmaniasis (*Leishmania* spp.), sleeping sickness (*Trypanosoma brucei* ssp.), and Chagas disease (*T. cruzi*) (Kostygov et al., 2021; Maslov et al., 2019; Stuart et al., 2008). In addition to the medical importance, some trypanosomatid parasites can infect plants or economically valued insects, such as honeybees (Frolov et al., 2021; Strobl et al., 2019; Tiritelli et al., 2025). The latter group of species has recently attracted increased research attention due to the harmful effects that some of these trypanosomatids have on honeybee and bumblebee populations (Gómez-Moracho et al., 2020; Liu et al., 2020; Schmid-Hempel et al., 2018; Schwarz et al., 2015). In line with this, substantial efforts are now being invested into the development of anti-trypanosomatid drugs that can be used in hymenopterans (Palmer-Young et al., 2022; Yuan et al., 2024). One of the proposed potential drugs is callunene, a volatile compound recently purified from the heather (*Calluna vulgaris*) nectar using semi-preparative high-performance liquid chromatography (HPLC) and identified as 4-(3-oxobut-1-enylidene)-3,5,5-trimethylcyclohex-2-en-1-one. This potent secondary metabolite was shown to suppress infectivity of *Crithidia bombi* in the bumblebee *Bombus terrestris*, explained by flagellum removal, which prevents attachment of these flagellates to the host's ileum wall and, thereby, makes gut colonization impossible (Koch et al., 2019). The precise mode of action and specific targets of callunene have not been investigated, warranting further research that could potentially lead to the development of new drugs against these important parasites.

The recent success in synthesizing callunene (Ferenczei et al., 2025) has prompted us to investigate its effects in different species

* Corresponding authors at: Department of Organic Chemistry, Faculty of Chemical Technology, University of Chemistry and Technology, 166 28 Prague, Czechia (P. Perlíková) and Life Science Research Centre, Faculty of Science, University of Ostrava, 710 00 Ostrava, Czechia (V. Yurchenko).
E-mail addresses: pavla.perlikova@vscht.cz (P. Perlíková), vyacheslav.yurchenko@osu.cz (V. Yurchenko).
[1] Equal contribution

https://doi.org/10.1016/j.ijpara.2025.12.002
0020-7519/

of Trypanosomatidae. Here we present results of these analyses in *C. bombi*, promastigotes and axenic amastigotes of *L. mexicana*, as well as procyclic and bloodstream forms of *T. brucei* (PF and BSF, respectively). The choice of analyzed species was determined by the following considerations: the effect of callunene was demonstrated in the first species (Koch et al., 2019), while the other two are medically relevant parasites representing distant trypanosomatid lineages (Albanaz et al., 2023; Kostygov et al., 2024a).

2. Materials and methods

2.1. Trypanosomatid cultures

The species identity was validated as described previously (Votýpka et al., 2012; Yurchenko et al., 2008).

Crithidia bombi isolate 5A (Klocek et al., 2023) was cultivated at 28 °C with 5 % CO_2 in M199 medium pH 5.5 (Sigma-Aldrich/Merck, Darmstadt, Germany), supplemented with 2 μg/ml biopterin (Merck), 2 μg/ml Hemin (Jena Bioscience, Jena, Germany), 25 mM HEPES (VWR/Avantor, Radnor, USA), 50 units/ml of penicillin, 50 μg/ml of streptomycin (both from Thermo Fisher Scientific, Waltham, USA), and 10 % heat-inactivated fetal bovine serum (FBS, BioSera, Nuaillé, France).

Leishmania mexicana isolate MNYC/BZ/1962/M379 was cultivated in the M199 medium with supplements listed above at pH 7.4 as described elsewhere (Durante et al., 2020). Amastigotes were differentiated and maintained in culture according to the previously established protocol (Bates, 1994; Ishemgulova et al., 2017).

Trypanosoma brucei procyclic (PF, line SmOxP927) and bloodstream (BSF, line SmOx2B427) forms (Poon et al., 2012) were cultivated in SDM-79 medium (Thermo Fisher Scientific) supplemented with 10 % FBS at 28 °C and HMI-11 medium (Thermo Fisher Scientific) supplemented with 10 % FBS at 37 °C in the presence of 5 % CO_2, respectively.

2.2. Synthesis of callunene and its derivatives

The synthesis of callunene and its analogs was based on a previously published approach (Ferenczei et al., 2025). Detailed information on the corresponding procedures along with characterization of the obtained compounds are presented in the Supplementary File 1.

2.3. Cell viability assay (Trypanosomatids)

A total of 10^6 cells/ml were seeded in 96-well plates and incubated in 2-fold dilution series of callunene or its derivatives with final concentrations ranging from 1,000 to 7.8 μM (100 and 0.78 μM for *T. brucei* bloodstream form) for 24 h. The cytotoxic effect of each compound was assayed using the colorimetric method based on the reduction of resazurin (alamarBlue, Thermo Fisher Scientific) by live cells (Mikus and Steverding, 2000). The fluorescence intensity was measured on the Infinite 200 Pro M Nano spectrophotometer (Tecan, Männedorf, Switzerland) at 570 nm (reduced form) and 600 nm (oxidized form). The data were analyzed using Prism v. 9 (GraphPad Software, San Diego, USA) with nonlinear regression to calculate IC_{50} values (±standard deviation, 95 % confidence intervals). Callunene concentrations of 30 and 60 μM were selected for all further analyses except for *T. brucei* bloodstream form experiments, in which 3 and 6 μM concentrations were used. Nifurtimox (Sigma-Aldrich/Merck), a nitrofuran derivative currently used in the treatment of Chagas disease and the sleeping sickness (Barrett, 2025; Cantizani et al., 2021), was used as a positive control. All experiments were performed in triplicates.

2.4. Cell viability assay (mammalian cells)

Human lung fibroblasts (cell line MRC-5) and human adult dermal fibroblasts (cell line HDF) were obtained from Merck and Thermo Fisher Scientific, respectively. Cells were cultivated in HEPES-free StableCell Minimum Essential Medium supplemented with 10 % FBS and 1 % non-essential amino acids (MRC-5) and Dulbecco′s modified Eagle′s medium with 10 % FBS (HDF) at 37 °C and 5 % CO_2. To assess the cytotoxicity of callunene and nifurtimox, cells were seeded into 96-well plates at the density of 1×10^4 per well, kept for 1 day, and treated with the tested compounds at concentrations ranging from 0 to 100 μM for 24 h. Subsequently, cells were washed in 1 × PBS and treated with WST-1 reagent (1:20, Merck) in 100 μl of phenol red-free culture media for 2 h. Absorbance of the resulting formazan product was measured at 450 nm on a Sunrise spectrophotometer (Tecan). All experiments were performed in triplicates. The data were analyzed using Prism software as above.

2.5. Microscopy and morphometry

Morphometric parameters were measured as described previously (Wheeler et al., 2011). In short, trypanosomatid cells were fixed with 4 % paraformaldehyde for 15 min in 1 × phosphate-buffered saline (PBS) at room temperature (RT) and permeabilized with 1 % Triton X-100 (Thermo Fisher Scientific). For immunofluorescence microscopy, trypanosomatid flagella were visualized with anti-polyglutamate (diluted 1:5,000, binding to polyglutamate chains on flagellar tubulin) and L8C4 (diluted 1:200, staining paraflagellar rod) antibodies [both kindly provided by Dr. Bastien, Institut Pasteur] as described previously (Kohl et al., 1999; Rogowski et al., 2010; Shang et al., 2002). Further, trypanosomatid cells were mounted in 4′,6-diamidino-2-phenylindole (DAPI)-containing medium (Thermo Fisher Scientific) and observed using a BX-53 microscope (Olympus, Tokyo, Japan) equipped with the DP73 digital camera. Images were taken with the cellSens v. 1.6 software (Olympus), then merged for multichannel visualization and analyzed in ImageJ v. 1.51 (Schneider et al., 2012). For direct detection of biotinylated callunene, *C. bombi* cells were incubated with Alexa Fluor 488-conjugated streptavidin (Thermo Fisher Scientific, diluted 1:1,000) for 1 h at RT and examined as above.

The statistical analyses were performed in Statistica v. 13.5.0.17 (TIBCO, Santa Clara, USA) with visualization in GraphPad Prism v. 9 (GraphPad Software/ Dotmatics, Boston, USA). The Mann-Whitney U and Wald-Wolfowitz tests were applied to morphometry data. Binomial confidence intervals for proportions were calculated using the "exact" Clopper–Pearson method (Clopper and Pearson, 1934). Comparisons of proportions were performed using the "N – 1" χ^2 test (Campbell, 2007).

2.6. Pull-down of biotinylated callunene and mass spectrometry analysis

Fifty million *C. bombi* cells were harvested and resuspended in 100 μl of a lysis buffer (50 mM Tris-HCl pH7.4, 150 mM NaCl, 0.1 % sodium dodecyl sulfate (SDS), 0.5 % Na-deoxycholate, 1 % NP-40, 1 mM EDTA) supplemented with the protease inhibitors cocktail (all reagents from Sigma-Aldrich/Merck). Lysates were incubated either with 1 mM of biotinylated callunene or biotin in the binding buffer (20 mM HEPES pH7.4, 10 mM $MgCl_2$, 0.1 mM DTT) for 30 min at 25 °C. The soluble protein fractions were then incubated with 15 μl of pre-equilibrated Dynabeads MyOne Streptavidin C1 coated magnetic beads (Thermo Fisher Scientific) for 2 h at 4 °C. The beads were washed thrice in the washing buffer (20 mM HEPES pH7.4, 10 mM $MgCl_2$, 0.1 mM DTT, 0.1 % NP-40) supplemented with protease inhibitors. Small aliquots of both

pull-downs were separated by PAGE and silver-stained to evaluate the quality. All experiments were performed in biological triplicates.

Eluted samples from the beads were resuspended in 20 % SDS (Thermo Fisher Scientific) and incubated at 50 °C for 20 min, followed by a reduction step with DTT at a final concentration of 100 mM for 15 min at 95 °C and processing *via* filter-aided sample preparation protocol (Wiśniewski, 2018). The obtained proteins were alkylated with iodoacetamide, incubated with trypsin for 18 h at 37 °C, and resuspended in 15 µl of 0.1 % formic acid. For proteomic analysis, the eluted peptides were separated by C18 reversed-phase chromatography on the UltiMate 3000 RSLCnano coupled with the Fusion Lumos Mass Spectrometer (both from Thermo Fisher Scientific) in an optimized 134 LC gradient. The MS/MS spectra after HCD fragmentation were recorded in Orbitrap analyzer (Thermo Fisher Scientific) at the resolution 30,000 at 200 *m*/*z* using a Data Independent Acquisition (DIA) mode in the precursor *m*/*z* range of 400–850.

The raw DIA LC-MS data were processed with DIA-NN v. 1.8 (Demichev et al., 2020) in a library-free search mode using the predicted proteome of *C. bombi* (NCBI GCA_900240985.1), *C. fasciculata* (NCBI GCA_000331325.2), and a cRAP database v. 1.8.1 (https://www.thegpm.org/crap/) to filter out common contaminants. The false discovery rate (FDR) thresholds were set at 1 % for both precursor and protein levels; a minimum number of proteolytic peptides threshold was set at 1.

2.7. Gene Ontology (GO) and ortholog analyses

GO enrichment analyses for the differentially expressed genes were performed in TriTrypDB release 68 (Shanmugasundram et al., 2023) using a *p*-value cutoff of 0.05. *Trypanosoma brucei* orthologs were identified using the same database and their localization was analyzed in the TrypTag (Billington et al., 2023; Sunter et al., 2023).

2.8. Phylogenetic analyses

NIPSNAP protein homologs were searched in the genomic dataset of Kinetoplastea taken from previous studies (Albanaz et al., 2023; Kostygov et al., 2024b) using the amino acid sequence of *C. bombi* NIPSNAP (*Cbom*_Cb.1.19010) as a query. The searches were performed by BLASTp against predicted proteomes (when available) and tBLASTn against genome assemblies with e-value threshold of 10^{-5}. The results were mapped to a cladogram of Trypanosomatidae (Kostygov et al., 2024a).

The collected amino acid sequences were aligned in MAFFT v. 7.520 (Katoh and Standley, 2013) using L-INS-I algorithm and BLOSUM45 substitution matrix. The alignment was trimmed with trimAl v. 1.5 (Capella-Gutiérrez et al., 2009) using a gap threshold of 0.5. Maximum likelihood analysis was performed in IQ-TREE v. 2.3.6 (Minh et al., 2020) under the automatically selected Q.Plant + I + G4 model with branch support estimated using 1,000 ultrafast bootstrap replicates. Bayesian inference was carried out in MrBayes v. 3.2.7 (Ronquist et al., 2012) under the LG + I + G model for 1,000,000 generations with every 100th of them sampled and other parameters set by default.

2.9. Transmission electron microscopy (TEM)

Trypanosomatid cells were fixed with 2.5 % glutaraldehyde in 0.1 M sodium cacodylate buffer (pH 7.4), washed with 1 × PBS, and post-fixed with 1 % osmium tetroxide for 2 h at RT as described previously (Yurchenko et al., 2014). The samples were then washed with 1 × PBS, dehydrated in a graded series of ethanol (30, 50, 70, 80, 90, 95 and 100 % for 15 min each) and infiltrated with a resin/acetone mixture at sequential ratios of 1:2, 1:1, and 2:1, each for 1 h. This was followed by overnight incubation in pure resin under vacuum in a desiccator and polymerization at 62 °C for 48 h. Ultrathin sections prepared using an Ultracut UCT microtome (Leica Biosystems, Nussloch, Germany) were stained with alcoholic uranyl acetate for 30 min and, then, by lead citrate for 20 min. Images were taken using a 1400 Flash transmission electron microscope (JEOL, Tokyo, Japan). The number of acidocalcisomes was quantified from longitudinal TEM cell sections.

2.10. Measurement of cellular ROS (Reactive Oxygen Species)

To estimate the level of ROS, 1×10^6 *C. bombi* cells were incubated with 30 and 60 µM of callunene for 24 h. Then, approximately 5×10^6 cells in exponential phase of growth were harvested for 5 min at 18,000 × g and the cell pellet was resuspended in 1 ml of fresh medium containing 10 µg/ml of 2′,7′-dichlorodihydrofluorescein diacetate (DCFH-DA, Sigma-Aldrich/Merck) for 1 h at 17 °C. After incubation, cells were washed twice with 1 × PBS, fixed in 4 % paraformaldehyde on poly-lysine adhesion slides, stained with DAPI and analyzed as above in ImageJ. At least 300 cells per condition were examined. Statistical analyses (Mann-Whitney U and Wald-Wolfowitz tests) were performed as above.

2.11. In silico prediction of callunene binding to NIPSNAP protein

The structure of *C. bombi* NIPSNAP protein was predicted using Chai-1 (Discovery, 2024). As a control, a homology model based on the solved crystal structure of NIPSNAP from *Paraburkholderia xenovorans* (PDB: 5K9F) as the template, was constructed using the Molecular Operating Environment v. 2024.0601 (Chemical Computing Group ULC, Montreal, Canada), showing a good agreement between the homology model and the co-folded structure. The binding site identified by Chai-1 was confirmed using the Site Finder tool from the Molecular Operating Environment and P2Rank v. 2.5 (Krivák and Hoksza, 2018), accessed via its web server. Molecular docking was employed to structurally validate binding of callunene and its derivatives to NIPSNAP (Paggi et al., 2024) using AutoDock Vina v. 1.2.0 (Eberhardt et al., 2021) and Molecular Operating Environment. Detection and visualization of Protein-Ligand interactions was done using Protein-Ligand Interaction Profiler (PLIP (Salentin et al., 2015)) and PyMOL Molecular Graphics System v. 3.0 (Schrödinger, New York, USA).

3. Results

3.1. Sensitivity of trypanosomatids to callunene and its cytotoxic effect against human fibroblasts

It has been recently shown that callunene purified from heather nectar is racemic and, therefore, identical to that produced by chemical synthesis (Ferenczei et al., 2025). Only the latter one was used throughout this study. Our analysis showed that IC_{50} value of callunene in *C. bombi* is ~40 µM (Table 1) after 24 h treatment contrasting with the previously reported value of ~110 µM (Koch et al., 2019). The discrepancy in the values can be attributed to differences in cultivation conditions and incubation times between two experimental settings, although the influence of other factors cannot be ruled out.

Callunene is similarly effective against *L. mexicana* (both procyclic promastigotes and axenically differentiated amastigotes) and *T. brucei* PF (Table 1). Of note, the IC_{50} value of callunene against *T. brucei* BSF was an order of magnitude lower (~5 µM). This value was comparable to that for nifurtimox (a clinically

Table 1
Antiparasitic activity of callunene and nifurtimox against different species of Trypanosomatidae and cytotoxic activity against selected noncancerous human cell lines. The IC_{50} values (mean ± standard deviation) are from three independent experiments.

Trypanosomatid species or human cells	IC_{50}, μM	
	Callunene	Nifurtimox
C. bombi	38.9 ± 11.1	6.7 ± 2.1
L. mexicana (promastigote)	53.1 ± 15.8	4.7 ± 0.7
L. mexicana (amastigote)	37.7 ± 10.9	19.2 ± 0.8
T. brucei (procyclic form)	42.0 ± 9.9	45.7 ± 10.7
T. brucei (bloodstream form)	5.1 ± 1.4	8.6 ± 0.9
HDF-1 (human dermal fibroblasts)	26.8 ± 8.0	>100
MRC-5 (human lung tissue-derived fibroblasts)	31.3 ± 9.0	>100

approved drug for treatment of Chagas disease and African trypanosomiasis) against the procyclic promastigotes of *L. mexicana* and BSF *T. brucei* (Barreiro-Costa et al., 2022; Enanga et al., 2003; Vincent et al., 2012). We concluded that the callunene's effect on trypanosomatids is neither limited to *C. bombi* nor species-specific.

Next, the effect of different concentrations of callunene on cell morphology was assessed in selected species of Trypanosomatidae (Supplementary Fig. S1). Consistent with the previous report (Koch et al., 2019), the compound caused dose-dependent flagellum shortening in *C. bombi*, a pattern also observed in promastigotes of *L. mexicana*. Notably, this effect was less pronounced in the procyclic or bloodstream forms of *T. brucei*, although other traits were clearly affected (Supplementary Fig. S1). These observations further reaffirm the conclusion that the effects of callunene on trypanosomatids are not species-specific.

The most striking previously reported phenotypic effect of callunene in *C. bombi* was the appearance of aflagellated cells (Koch et al., 2019). To assess whether their proportions differ between *C. bombi* and *L. mexicana* promastigotes in untreated and callunene-treated conditions (Supplementary Fig. S2), flagella were visualized using immunofluorescence microscopy. In all conditions tested, the proportion of aflagellated cells in *C. bombi* was significantly higher (χ^2 test: 0 μM: χ^2 (df = 1, N = 360, 439) = 136.9, p = 1.27e^{-31}); 30 μM: χ^2 (df = 1, N = 356, 362) = 44.7, p = 2.25e^{-11}); 60 μM: χ^2 (df = 1, N = 458, 283) = 14.1, p = 1.73e^{-04}). In both species, the proportion of aflagellated cells increased in a dose-dependent manner with higher callunene concentrations.

Leishmania mexicana and *T. brucei* are responsible for serious diseases in humans. Given the callunene activity against these parasites, its cytotoxicity against human fibroblasts (HDF, MRC-5) was evaluated. Selectivity for trypanosomatids'- over the host cells' is a critical factor in assessing a compound's potential as a hit for further therapeutic development. The cytotoxic activity of callunene after 24 h treatment was comparable between trypanosomatids and human fibroblasts, except for the BST *T. brucei*, in which the effect on the parasites was more pronounced than against the human cells (Table 1). However, the selectivity index remained low (SI = 6.1; calculated as the ratio of IC_{50} for MRC-5 to IC_{50} for *T. brucei* BSF). Under the same conditions, nifurtimox showed no toxic effect against human fibroblasts (IC_{50} over 100 μM). Since the cytotoxicity of callunene limits its direct application in treatment of trypanosomatid infections in humans or cattle, further experiments focused exclusively on its effects in *C. bombi*.

3.2. Sensitivity of C. bombi to callunene derivatives

To identify structural moieties responsible for the biological activity of callunene (Fig. 1, compound **1a**) and suitable sites for biotin labeling, a series of callunene analogs were synthesized (Supplementary File 1) and tested for cytotoxic activity against *C. bombi* (Table 2).

We first explored substitutions at the methyl group of the callunene side chain (compounds **1b**–**d**). The activity has slightly improved when the side chain was extended by two carbons (compound **1b**). However, further elongation of the side chain resulted in a decrease in activity (compound **1c**). Nevertheless, substituting the methyl group with a phenyl group (compound **1d**) led to only a slight loss of activity compared to that of callunene. The contribution of the keto groups was investigated by converting them into hydroxy groups. Each keto group was studied separately, with the keto group in the side chain being converted into either a secondary- or a tertiary alcohol (compound **2a** and **2b**, respectively). Substitution of the allenic moiety by a hydroxyalkyne group (compound **3**) also decreased cytotoxicity of the resulting derivate. Compound **4** was used to assess the role of the keto group in the cyclohexanone moiety. The corresponding alcohols **2a**–**b** and **4** exhibited substantially higher IC_{50} values compared to that of callunene, confirming the importance of the keto groups for activity.

Results of the activity were used to design a biotinylated molecule, in which the biotin tag was attached to the side chain of callunene. The resulting compound **5** exhibited an IC_{50} approximately twice that of the callunene (Table 2) and was, therefore, considered suitable for downstream analyses.

3.3. Identification of putative callunene targets

The biotinylated callunene (Fig. 1, compound **5**) was used to pull down its putative interaction partners in *C. bombi*. Using Alexa Fluor 488-conjugated streptavidin, internalization of the compound by the flagellates was confirmed (Fig. 2A), justifying downstream analysis. Indeed, examination using gel electrophoresis (Fig. 2B) followed by mass spectrometry (Fig. 2C) revealed 56 proteins overrepresented (over 2.8-fold with adjusted *p*-value below 0.05) in the pull-down fractions of biotinylated callunene compared to the biotin-only control (Supplementary Table S1). Among these 56 candidates, 19 were conserved hypothetical proteins and 16 had no orthologs in *T. brucei*.

The most notable candidate was a homolog of NIPSNAP proteins. In other model systems including vertebrates, the NIPSNAP proteins have been implicated in mitophagy (autophagy of damaged mitochondria) (Fathi et al., 2021; Princely Abudu et al., 2019), and this function appears to be preserved in at least some trypanosomatids, suggesting that callunene acts by modulating the function of mitochondria in *C. bombi* (of note, the mechanism of callunene action in these species possessing a single mitochondrion must differ from that in other model organisms). This hypothesis is further supported by GO analysis of the callunene-bound targets, which showed significant enrichment of mitochondrial proteins involved in oxidoreductase and glutathione dehydrogenase activities, as well as NAD/NADPH and cation binding. Furthermore, *T. brucei* orthologs of many of these proteins localize to the single reticulated mitochondrion (Supplementary Table S1).

3.4. NIPSNAP

Because NIPSNAP was by far the most overrepresented candidate with clear implication for a possible biological function, it was investigated further. A search for homologs of this protein in the representative dataset (Kostygov et al., 2024a) returned single-copy genes for the majority of species within Trypanosomatidae, but none for the salivarian trypanosomes (*Trypanosoma* (*Trypanozoon*) *brucei* ssp., *T.* (*Nannomonas*) *congolense*, and *T.* (*Duttonella*) *vivax*), the piscine parasite *Trypanosoma boissoni*, and the monoxenous *Vickermania* spp. Among outgroups, the protein was

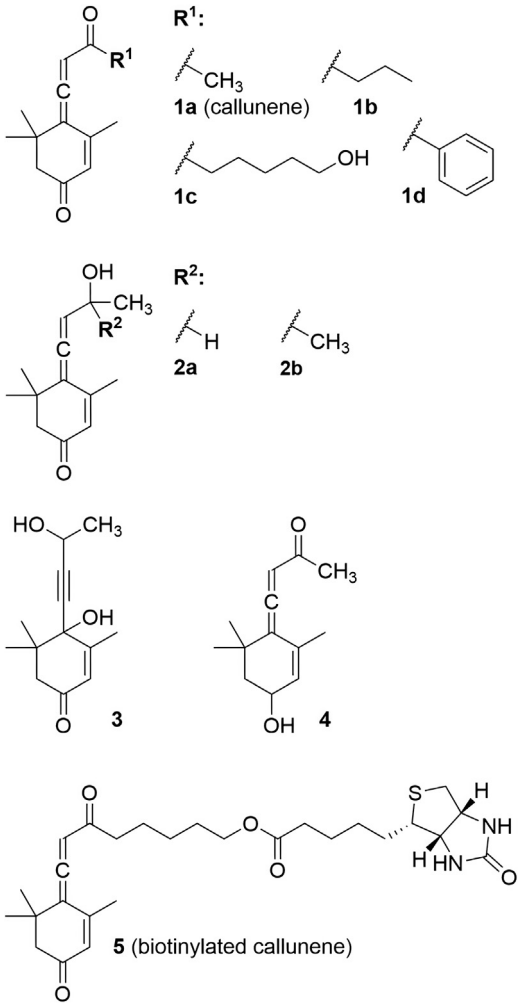

Fig. 1. Chemical structure of callunene and its synthetic derivatives. **1a**, parent callunene; **1b–d**, side-chain modifications (methyl extension or phenyl substitution); **2a–b**, conversion of the terminal keto group to secondary or tertiary alcohol; **3**, allenyl ketone isomerized to hydroxyalkyne; **4**, keto-group reduction in the cyclohexanone ring; **5**, biotinylated derivative.

found only in the free-living *Bodo saltans*, the closest known relative of the family Trypanosomatidae (Fig. 3).

The length of the protein is rather conserved being around 200 amino acids, with the shortest one documented in *Jaenimonas drosophilae* and the longest one – in *Blastocrithidia nonstop* (194 and 220 amino acids, respectively). The fact that it was longer in *B. nonstop* is not surprising, as proteins of Blastocrithidiinae are known to harbor numerous insertions that do not seem to interfere with their function or structure (Afonin et al., 2024; Nenarokova et al., 2019). The identity levels of NIPSNAPs within trypanosomatids ranged from 31.37 % between *T. marinkellei* and *Phytomonas francai* to 100 % between closely related *Leishmania guyanensis* and *L. panamensis*. The protein from *Bodo saltans* was the most divergent one in the dataset showing only 18.36–33.17 % identity to those of trypanosomatids. NIPSNAP was not identified in more distantly related *Trypanoplasma* and *Perkinsela* spp. (Fig. 3). Phylogenetic analysis of the NIPSNAP orthologs demonstrated uneven evolutionary rates among lineages with the longest branches leading to the plant-parasitic *Phytomonas* spp. and the monoxenous insect-infecting *Wallacemonas* spp. (Supplementary Fig. S3). Topology was generally correct within the terminal clades, as judged by the most comprehensive phylogenomic inference available (Kostygov et al., 2024a). The only noticeable discrepancy was a position of *Kentomonas sorsogonicus* sequence placed far from its relatives *Angomonas* and *Strigomonas* spp. (Motta et al., 2025; Votýpka et al., 2014). This can likely be explained by the high divergence of the sequence in that particular endosymbiont-bearing trypanosomatid.

A consensus-based approach was applied to analyze binding of callunene to NIPSNAP of *C. bombi*. This identified a putative binding pose, in which callunene forms hydrogen bonds with Gln67 and Arg81 of the protein (Fig. 4, of note, Gln and Arg are predominant but not absolutely conserved in these positions among trypanosomatids). To further support this specific pose, constrained docking was performed on a series of callunene derivatives except for biotinylated callunene, which skewed the docking score because of its significantly higher molecular weight. The docking scores of the derivatives correlated well with their measured IC_{50} (Pearson correlation coefficient = –0.86; $p = 0.006$; Spearman's rank correlation coefficient = –0.88; $p = 0.0038$), supporting the identified pose. *In silico* analysis of callunene binding to the NIPSNAP of *L. mexicana* (72.5 % pairwise identity to the *C. bombi* ortholog) demonstrated a good overlay of both residues Gln67 and Arg81 potential binding sites (RMSD 1.10 Å) and of the overall pose (RMSD 1.65 Å). This further supports the conclusion that the mode of callunene action is not species-specific, as the compound can efficiently bind to NIPSNAP proteins of different trypanosomatid species.

3.5. Consequences of callunene treatment: modulation of mitophagy and mitochondrial metabolism

Results presented in the previous section suggested that callunene may act on the *C. bombi* mitochondrion, as NIPSNAP proteins are known to induce mitophagy and modulate mitochondrial metabolism. Since acidocalcisomes are known as key players in trypanosomatid autophagy (Li and He, 2014, 2017), we used TEM to estimate their number *per* cell upon the callunene treatment (Fig. 5). Indeed, treatment with callunene significantly increased the number of acidocalcisomes in *C. bombi*. It is

Table 2
Antiparasitic activity of callunene derivatives in *C. bombi*. The IC_{50} values (in μM, mean ± standard deviation) are from three independent experiments. Results of the Welch's one-tailed *t*-test are shown on the right.

Compound	IC_{50} ± SD, μM	Welch's one-tailed *t*-test		
		approx. df	*t*-value	*p*-value
1a (callunene)	38.9 ± 11.1	–	–	–
1b	23 ± 5.5	3	–2.223	0.091
1c	71 ± 23.5	3	2.139	0.100
1d	48 ± 11.1	4	1.004	0.186
2a	78.1 ± 14.1	4	3.784	0.009
2b	381.4 ± 17.5	3	28.63	2.7e-06
3	181.3 ± 86.3	2	2.835	0.064
4	127.3 ± 36.1	2	4.054	0.028
5	88.9 ± 14.4	4	4.763	0.004

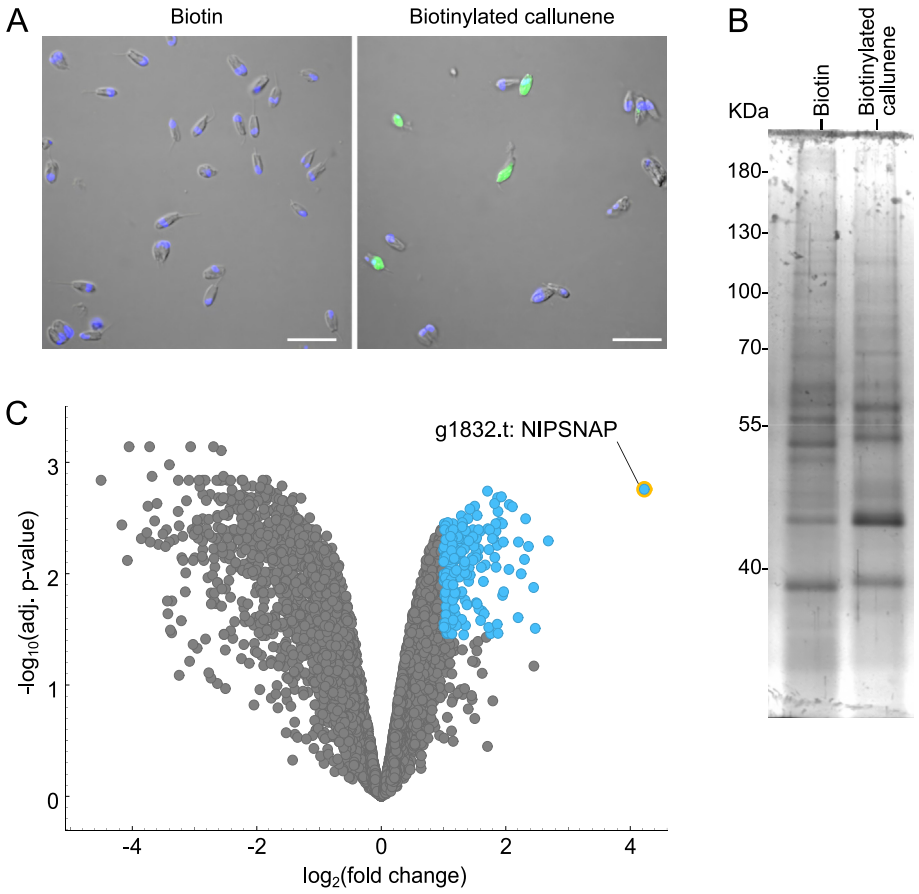

Fig. 2. Identification of potential targets of callunene. (A) Biotinylated callunene inside *C. bombi* cells, visualized with streptavidin-Alexa 488 (green) and DAPI (blue). Scale bar, 10 µm. (B) Pull-down of *C. bombi* proteins using biotin or biotinylated callunene, visualized by silver staining after PAAG separation. Molecular weight marker sizes (kDa) are indicated on the left. (C) Volcano plot of identified candidate proteins. Highly confident hits (log_2 fold change >1.5 and adjusted *p*-value <0.05) are in light blue. The NIPSNAP homolog is marked. (For interpretation of the references to color in this figure legend, the reader is referred to the web version of this article.)

tempting to speculate that acidocalcisomes may also participate in regulating mitophagy, thereby linking this process to NIPSNAP function. This hypothesis is indirectly supported by the recent analysis of contact sites between acidocalcisomes and kinetoplasts in Trypanosomatidae (Ramakrishnan et al., 2018).

Next, we analyzed ROS levels in *C. bombi* upon callunene treatment. As expected, they positively correlated with a drug concentration (Fig. 6) further validating our conclusion that callunene affects mitochondrial metabolism in Trypanosomatidae.

Taken together, these findings indicate that callunene interferes with mitophagy in *C. bombi* supporting a previously posited idea that mitochondrion and mitochondrial proteins are promising drug target in trypanosomatid parasites (Fidalgo and Gille, 2011; Pedra-Rezende et al., 2022).

4. Discussion

Callunene (4-(3-oxobut-1-enylidene)-3,5,5-trimethylcyclohex-2-en-1-one), a volatile secondary metabolite recently isolated from heather nectar, has been implicated in flagellum removal in *Crithidia bombi*, resulting in inability of the parasites to colonize bumblebees (Koch et al., 2019).

The first question posed in this study concerned callunene specificity across different trypanosomatid species. The compound showed similar in vitro efficacy against *C. bombi*, *L. mexicana*, and PF *T. brucei*, which together cover a broad spectrum of Trypanosomatidae. Flagellar removal, previously reported in *C. bombi* and showcased as an intriguing and novel phenotype (Koch et al., 2019), could have placed callunene alongside other compounds demonstrated to specifically target the trypanosomatid flagellum of these mono-flagellated protists (da Silva et al., 2021; Santos et al., 2023). Our data showed that flagellar shortening was not restricted to *C. bombi*, as a similar effect was documented in *L. mexicana*. This phenomenon may be linked to the fact that aflagellate forms of trypanosomatids (termed amastigotes or endomastigotes in different species) are typically more resistant to adverse environmental conditions (Frolov et al., 2021; Jara et al., 2022; Saunders et al., 2021). Thus, the formation of such cells in response to callunene may represent a common survival strategy. In any case, similar sensitivity to callunene across analyzed trypanosomatids (except for BSF *T. brucei* discussed below) confirms that its mechanism of action is general. Nevertheless, the molecular details of the flagellar detachment (for example, interactions with proteins involved in flagellar assembly/depolymerization) warrant further investigation.

Callunene exhibits antiparasitic activity comparable to that of nifurtimox against *T. brucei*, but cytotoxicity toward human fibroblasts precludes its direct therapeutic use in medicine. In addition to identifying the NIPSNAP protein as a potential target in pull-down assays, the antiparasitic activity data align with the results of

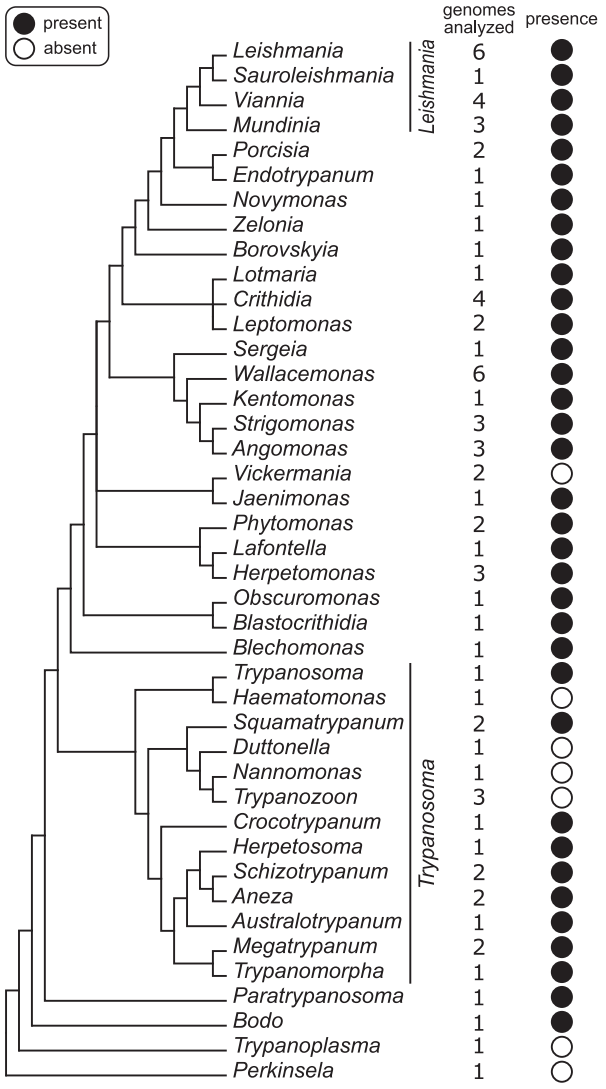

Fig. 3. NIPSNAP presence (filled circles) and absence (open circles) in different lineages of Kinetoplastea. For the genera *Leishmania* and *Trypanosoma*, recognized subgenera are shown.

molecular docking studies. The oxo groups of callunene are key structural features for maintaining activity and, indeed, mediate binding to NIPSNAP. Given the high conservation of NIPSNAP proteins, it is plausible that callunene affects both trypanosomatid and human mitochondria, contributing to the limited selectivity observed. However, testing this hypothesis goes beyond the scope of the present study.

The exact role of NIPSNAP in trypanosomatid mitophagy remains unclear, given that these flagellates invariably possess a single mitochondrion per cell. However, it forms an extensively branching, interconnected network dynamically remodeled throughout the life cycle (Bílý et al., 2021). Mitophagy may play a crucial role in this process, with NIPSNAP serving as a potential regulator. The observed effect of callunene on the abundance of acidocalcisomes—organelles associated with autophagy—likely represents the link to mitophagy. In multicellular organisms, NIPSNAP proteins have been shown to modulate mitochondrial metabolism and participate in processes such as pain transmission, neurological function, and cancer signaling (Fathi et al., 2021; Princely Abudu et al., 2019).

Although NIPSNAP appears to be involved in the mode of callunene's action in both *C. bombi* and *L. mexicana*, its antiparasitic effect was also observed in *T. brucei*, which lacks a gene encoding NIPSNAP. This suggests that, in addition to interacting with NIPSNAP, callunene may target other molecules (not identified in our pull-down assay) that are shared across the three tested trypanosomatid species. Identifying these additional targets remains an open question for future research. The elevated sensitivity of the bloodstream form of *T. brucei* may provide a clue in this regard, as this stage is physiologically distinct from the procyclic form and the other trypanosomatids studied in this work. For example, the BSF *T. brucei* does not contain a respiring electron transport chain potentially leading to the downregulation of anti-oxidant features in this life cycle stage and appearance of "extra-vulnerable" mitochondria.

In conclusion, the antiparasitic effect of callunene against trypanosomatids is not species-specific. However, its limited selectivity compromises its suitability for further antiparasitic drug development. Our findings demonstrate that callunene affects mitochondrial function, with NIPSNAP identified as a molecular target of callunene in *C. bombi*. Nevertheless, its activity against *T. brucei* lacking NIPSNAP indicates the existence of other targets in trypanosomatids. The additional cellular target remains to be

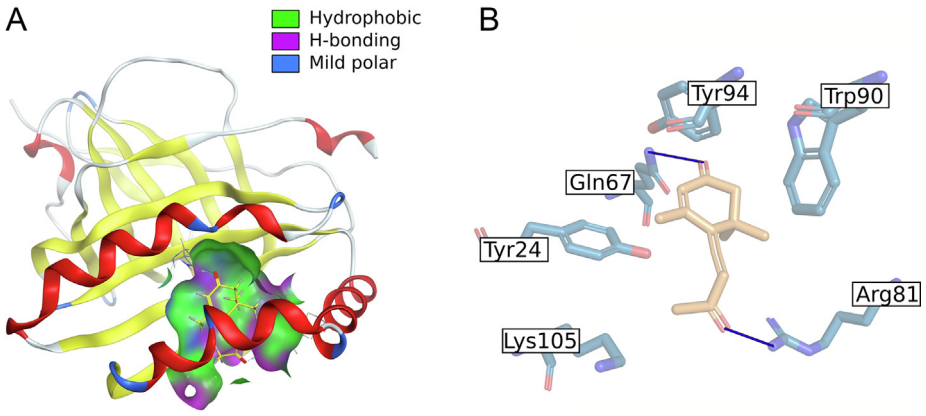

Fig. 4. (A) *Crithidia bombi* NIPSNAP protein structure with callunene in the binding pocket as predicted by Chai-1. (B) Amino acid residues forming the binding site. Arg81 and Gln67 participate in hydrogen bonding, the remaining residues are involved in hydrophobic interactions.

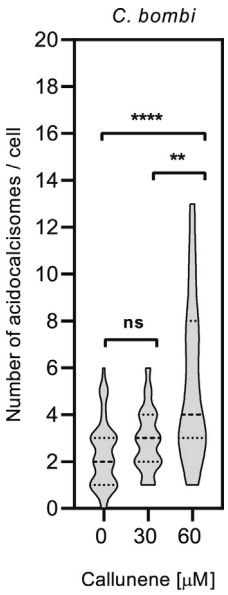

Fig. 5. Abundance of acidocalcisomes *per* longitudinal section of a cell.

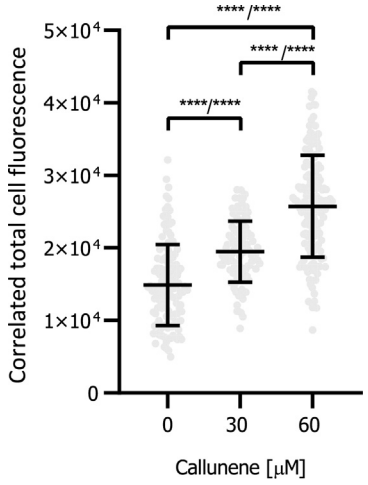

Fig. 6. Intracellular reactive oxygen species (ROS) after 24 h of 0, 30 and 60 μM callunene treatment. The error bars indicate standard deviation. Statistical significance (Wald-Wolfowitz and Mann-Whitney U tests) is shown by asterisks (**** symbolize *p*-values <0.0001).

identified. Despite these limitations, callunene represents a promising chemical probe for studying mitophagy in Trypanosomatidae or for controlling parasites in non-mammalian hosts (for example, honeybees). Given the challenges associated with monotherapy, the development of multi-target drugs is becoming increasingly important (Braga, 2019; Cavalli and Bolognesi, 2009; Gomes et al., 2024).

CRediT authorship contribution statement

Andreu Saura: Writing – original draft, Visualization, Validation, Investigation, Formal analysis, Data curation. **Vilém Blahout:** Investigation, Data curation. **Edubiel A. Alpizar-Sosa:** Writing – original draft, Visualization, Validation, Investigation, Formal analysis, Data curation. **Haoshen Wen:** Investigation, Validation. **Aditya Reddy:** Investigation. **Galina Prokopchuk:** Writing – review & editing, Investigation. **Julius Lukeš:** Writing – review & editing, Data curation. **Tereza Kubátová:** Investigation. **Wim Dehaen:** Writing – review & editing, Investigation, Formal analysis. **Silvie Rimpelová:** Writing – review & editing, Investigation. **Alexei Yu. Kostygov:** Writing – review & editing, Writing – original draft, Visualization, Validation, Supervision, Methodology, Investigation, Formal analysis, Data curation, Conceptualization. **Pavla Perlíková:** Writing – review & editing, Writing – original draft, Visualization, Validation, Supervision, Resources, Investigation, Funding acquisition, Formal analysis, Data curation, Conceptualization. **Vyacheslav Yurchenko:** Writing – review & editing, Writing – original draft, Visualization, Supervision, Resources, Project administration, Methodology, Funding acquisition, Data curation, Conceptualization.

Acknowledgments

This work was primarily supported by the European Union Operational Program "Just Transition" (LERCO CZ.10.03.01/00/22_003/0000003) to V.Y., A.S., E.A.-S., and A.Y.K. W.D. was supported by the Czech Ministry of Education, Youth and Sports under the program "National Infrastructure for Chemical Biology" (LM2023052 CZ-OPENSCREEN) co-funded by the European Union. W.D. and P.P. were supported by the project New Technologies for Translational Research in Pharmaceutical Sciences/NETPHARM (CZ.02.01.01/00/22_008/0004607) co-funded by the European Union. We also acknowledge the CEITEC proteomics core facility of CIISB Instruct-CZ Centre and the core facility of Biology Centre both supported by the Czech Ministry of Education, Youth and Sports (LM2023042, e-INFRA CZ 90254, LM2023050 CZ-BioImaging, and OP VVV CZ.02.1.01/0.0/0.0/18_046/0016045) as well as the European Regional Development Fund-Project „Innovation of Czech Infrastructure for Integrative Structural Biology" CZ.02.01.01/00/23_015/0008175. We thank members of our laboratories for stimulating discussion and technical assistance. We are also grateful to Dr. Bastien (Pasteur Institute) for providing primary antibodies used to visualize flagella.

Appendix A. Supplementary material

Supplementary material to this article can be found online at https://doi.org/10.1016/j.ijpara.2025.12.002.

References

Afonin, D.A., Gerasimov, E.S., Škodová-Sveráková, I., Záhonová, K., Gahura, O., Albanaz, A.T.S., Myšková, E., Bykova, A., Paris, Z., Lukeš, J., Opperdoes, F.R., Horváth, A., Zimmer, S.L., Yurchenko, V., 2024. *Blastocrithidia nonstop* mitochondrial genome and its expression are remarkably insulated from nuclear codon reassignment. Nucleic Acids Res. 52, 3870–3885.

Albanaz, A.T.S., Carrington, M., Frolov, A.O., Ganyukova, A.I., Gerasimov, E.S., Kostygov, A.Y., Lukeš, J., Malysheva, M.N., Votýpka, J., Zakharova, A., Záhonová, K., Zimmer, S.L., Yurchenko, V., Butenko, A., 2023. Shining the spotlight on the neglected: new high-quality genome assemblies as a gateway to understanding the evolution of Trypanosomatidae. BMC Genomics 24, 471.

Barreiro-Costa, O., Quiroga Lozano, C., Muñoz, E., Rojas-Silva, P., Medeiros, A., Comini, M.A., Heredia-Moya, J., 2022. Evaluation of the anti-*Leishmania mexicana* and -*Trypanosoma brucei* activity and mode of action of 4,4′-(arylmethylene)bis(3-methyl-1-phenyl-1*H*-pyrazol-5-ol). Biomedicines 10, 1913.

Barrett, M.P., 2025. Transforming the chemotherapy of human African trypanosomiasis. Clin. Microbiol. Rev. 38, e0015323.

Bates, P.A., 1994. Complete developmental cycle of *Leishmania mexicana* in axenic culture. Parasitology 108, 1–9.

Billington, K., Halliday, C., Madden, R., Dyer, P., Barker, A.R., Moreira-Leite, F.F., Carrington, M., Vaughan, S., Hertz-Fowler, C., Dean, S., Sunter, J.D., Wheeler, R.J., Gull, K., 2023. Genome-wide subcellular protein map for the flagellate parasite *Trypanosoma brucei*. Nat. Microbiol. 8, 533–547.

Bílý, T., Sheikh, S., Mallet, A., Bastin, P., Pérez-Morga, D., Lukeš, J., Hashimi, H., 2021. Ultrastructural changes of the mitochondrion during the life cycle of *Trypanosoma brucei*. J. Eukaryot. Microbiol. 68, e12846.

Braga, S.S., 2019. Multi-target drugs active against leishmaniasis: a paradigm of drug repurposing. Eur. J. Med. Chem. 183, 111660.

Campbell, I., 2007. Chi-squared and Fisher-Irwin tests of two-by-two tables with small sample recommendations. Stat. Med. 26, 3661–3675.
Cantizani, J., Gamallo, P., Cotillo, I., Alvarez-Velilla, R., Martin, J., 2021. Rate-of-Kill (RoK) assays to triage large compound sets for Chagas disease drug discovery: application to GSK Chagas Box. PLoS Negl. Trop. Dis. 15, e0009602.
Capella-Gutiérrez, S., Silla-Martinez, J.M., Gabaldon, T., 2009. trimAl: a tool for automated alignment trimming in large-scale phylogenetic analyses. Bioinformatics 25, 1972–1973.
Cavalli, A., Bolognesi, M.L., 2009. Neglected tropical diseases: multi-target-directed ligands in the search for novel lead candidates against *Trypanosoma* and *Leishmania*. J. Med. Chem. 52, 7339–7359.
Clopper, C., Pearson, E.S., 1934. The use of confidence or fiducial limits illustrated in the case of the binomial. Biometrika 26, 404–413.
da Silva, M.J.V., Jacomini, A.P., Goncalves, D.S., Pianoski, K.E., Poletto, J., Lazarin-Bidoia, D., Volpato, H., Nakamura, C.V., Rosa, F.A., 2021. Discovery of 1,3,4,5-tetrasubstituted pyrazoles as anti-trypanosomatid agents: Identification of alterations in flagellar structure of *L. amazonensis*. Bioorg. Chem. 114, 105082.
Demichev, V., Messner, C.B., Vernardis, S.I., Lilley, K.S., Ralser, M., 2020. DIA-NN: neural networks and interference correction enable deep proteome coverage in high throughput. Nat. Methods 17, 41–44.
Discovery, C., 2024. Chai-1: decoding the molecular interactions of life. BioRxiv. https://doi.org/10.1101/2024.1110.1110.615955.
Durante, I.M., Butenko, A., Rašková, V., Charyyeva, A., Svobodová, M., Yurchenko, V., Hashimi, H., Lukeš, J., 2020. Large-scale phylogenetic analysis of trypanosomatid adenylate cyclases reveals associations with extracellular lifestyle and host-pathogen interplay. Genome Biol. Evol. 12, 2403–2416.
Eberhardt, J., Santos-Martins, D., Tillack, A.F., Forli, S., 2021. AutoDock Vina 1.2.0: new docking methods, expanded force field, and python bindings. J. Chem. Inf. Model. 61, 3891–3898.
Enanga, B., Ariyanayagam, M.R., Stewart, M.L., Barrett, M.P., 2003. Activity of megazol, a trypanocidal nitroimidazole, is associated with DNA damage. Antimicrob. Agents Chemother. 47, 3368–3370.
Fathi, E., Yarbro, J.M., Homayouni, R., 2021. NIPSNAP protein family emerges as a sensor of mitochondrial health. Bioessays 43, e2100014.
Ferenczei, J., Blahout, V., Dvořáková, H., Brancale, A., Cuřínová, P., Labíková, M., Kohout, M., Setnička, V., Perlíková, P., 2025. Stereo-analysis of the antiparasitic natural product callunene and its synthetic intermediates. J. Nat. Prod. 88, 723–731.
Fidalgo, L.M., Gille, L., 2011. Mitochondria and trypanosomatids: targets and drugs. Pharm. Res. 28, 2758–2770.
Frolov, A.O., Kostygov, A.Y., Yurchenko, V., 2021. Development of monoxenous trypanosomatids and phytomonads in insects. Trends Parasitol. 37, 538–551.
Gomes, M.C., Padilha, E.K.A., Diniz, G.R.A., Gomes, E.C., da Silva Santos-Junior, P.F., Zhan, P., da Siva-Junior, E.F., 2024. Multi-target compounds against trypanosomatid parasites and *Mycobacterium tuberculosis*. Curr. Drug Targets 25, 602–619.
Gómez-Moracho, T., Buendía-Abad, M., Benito, M., García-Palencia, P., Barrios, L., Bartolomé, C., Maside, X., Meana, A., Jiménez-Antón, M.D., Olías-Molero, A.I., Alunda, J.M., Martín-Hernández, R., Higes, M., 2020. Experimental evidence of harmful effects of *Crithidia mellificae* and *Lotmaria passim* on honey bees. Int. J. Parasitol. 50, 1117–1124.
Ishemgulova, A., Kraeva, N., Hlaváčová, J., Zimmer, S.L., Butenko, A., Podešvová, L., Leštinová, T., Lukeš, J., Kostygov, A., Votýpka, J., Volf, P., Yurchenko, V., 2017. A putative ATP/GTP binding protein affects *Leishmania mexicana* growth in insect vectors and vertebrate hosts. PLoS Negl. Trop. Dis. 11, e0005782.
Jara, M., Barrett, M., Maes, I., Regnault, C., Imamura, H., Domagalska, M.A., Dujardin, J.C., 2022. Transcriptional shift and metabolic adaptations during *Leishmania* quiescence using stationary phase and drug pressure as models. Microorganisms 10, 97.
Katoh, K., Standley, D.M., 2013. MAFFT multiple sequence alignment software version 7: improvements in performance and usability. Mol. Biol. Evol. 30, 772–780.
Klocek, D., Grybchuk, D., Macedo, D.H., Galan, A., Votýpka, J., Schmid-Hempel, R., Schmid-Hempel, P., Yurchenko, V., Kostygov, A.Y., 2023. RNA viruses of *Crithidia bombi*, a parasite of bumblebees. J. Invertebr. Pathol. 201, 107991.
Koch, H., Woodward, J., Langat, M.K., Brown, M.J., Stevenson, P.C., 2019. Flagellum removal by a nectar metabolite inhibits infectivity of a bumblebee parasite. Curr. Biol. 29, 3494–3500.
Kohl, L., Sherwin, T., Gull, K., 1999. Assembly of the paraflagellar rod and the flagellum attachment zone complex during the *Trypanosoma brucei* cell cycle. J. Eukaryot. Microbiol. 46, 105–109.
Kostygov, A.Y., Albanaz, A.T.S., Butenko, A., Gerasimov, E.S., Lukeš, J., Yurchenko, V., 2024a. Phylogenetic framework to explore trait evolution in Trypanosomatidae. Trends Parasitol. 40, 96–99.
Kostygov, A.Y., Karnkowska, A., Votýpka, J., Tashyreva, D., Maciszewski, K., Yurchenko, V., Lukeš, J., 2021. Euglenozoa: taxonomy, diversity and ecology, symbioses and viruses. Open Biol. 11, 200407.
Kostygov, A.Y., Skýpalová, K., Kraeva, N., Kalita, E., McLeod, C., Yurchenko, V., Field, M.C., Lukeš, J., Butenko, A., 2024b. Comprehensive analysis of the Kinetoplastea intron landscape reveals a novel intron-containing gene and the first exclusively *trans*-splicing eukaryote. BMC Biol. 22, 281.
Krivák, R., Hoksza, D., 2018. P2Rank: machine learning based tool for rapid and accurate prediction of ligand binding sites from protein structure. J. Cheminform. 10, 39.
Li, F.J., He, C.Y., 2014. Acidocalcisome is required for autophagy in *Trypanosoma brucei*. Autophagy 10, 1978–1988.
Li, F.J., He, C.Y., 2017. Autophagy in protozoan parasites: *Trypanosoma brucei* as a model. Future Microbiol. 12, 1337–1340.
Liu, Q., Lei, J., Darby, A.C., Kadowaki, T., 2020. Trypanosomatid parasite dynamically changes the transcriptome during infection and modifies honey bee physiology. Commun. Biol. 3, 51.
Maslov, D.A., Opperdoes, F.R., Kostygov, A.Y., Hashimi, H., Lukeš, J., Yurchenko, V., 2019. Recent advances in trypanosomatid research: genome organization, expression, metabolism, taxonomy and evolution. Parasitology 146, 1–27.
Mikus, J., Steverding, D., 2000. A simple colorimetric method to screen drug cytotoxicity against *Leishmania* using the dye Alamar Blue. Parasitol. Int. 48, 265–269.
Minh, B.Q., Schmidt, H.A., Chernomor, O., Schrempf, D., Woodhams, M.D., von Haeseler, A., Lanfear, R., 2020. IQ-TREE 2: new models and efficient methods for phylogenetic inference in the genomic era. Mol. Biol. Evol. 37, 1530–1534.
Motta, M.C.M., Camelo, T.M., Cerdeira, C.M.C., Goncalves, C.S., Borghesan, T.C., Villalba-Aleman, E., de Souza, W., Teixeira, M.M.G., de Camargo, E.F.P., 2025. Phylogenetic and structural characterization of *Kentomonas inusitatus* n. sp.: unique insect trypanosomatid of the Strigomonadinae subfamily naturally lacking bacterial endosymbiont. J. Eukaryot. Microbiol. 72, e13083.
Nenarokova, A., Záhonová, K., Krasilnikova, M., Gahura, O., McCulloch, R., Zíková, A., Yurchenko, V., Lukeš, J., 2019. Causes and effects of loss of classical nonhomologous end joining pathway in parasitic eukaryotes. mBio 10, e01541-01519.
Paggi, J.M., Pandit, A., Dror, R.O., 2024. The art and science of molecular docking. Annu. Rev. Biochem. 93, 389–410.
Palmer-Young, E.C., Markowitz, L.M., Grubbs, K., Zhang, Y., Corona, M., Schwarz, R., Chen, Y., Evans, J.D., 2022. Antiparasitic effects of three floral volatiles on trypanosomatid infection in honey bees. J. Invertebr. Pathol. 194, 107830.
Pedra-Rezende, Y., Bombaca, A.C.S., Menna-Barreto, R.F.S., 2022. Is the mitochondrion a promising drug target in trypanosomatids? Mem. Inst. Oswaldo Cruz 117, e210379.
Poon, S.K., Peacock, L., Gibson, W., Gull, K., Kelly, S., 2012. A modular and optimized single marker system for generating *Trypanosoma brucei* cell lines expressing T7 RNA polymerase and the tetracycline repressor. Open Biol. 2, 110037.
Princely Abudu, Y., Pankiv, S., Mathai, B.J., Hakon Lystad, A., Bindesboll, C., Brenne, H.B., Yoke Wui Ng, M., Thiede, B., Yamamoto, A., Mutugi Nthiga, T., Lamark, T., Esguerra, C.V., Johansen, T., Simonsen, A., 2019. NIPSNAP1 and NIPSNAP2 act as "eat me" signals for mitophagy. Dev. Cell 49, 509–525.
Ramakrishnan, S., Asady, B., Docampo, R., 2018. Acidocalcisome-mitochondrion membrane contact sites in *Trypanosoma brucei*. Pathogens 7, 33.
Rogowski, K., van Dijk, J., Magiera, M.M., Bosc, C., Deloulme, J.C., Bosson, A., Peris, L., Gold, N.D., Lacroix, B., Bosch Grau, M., Bec, N., Larroque, C., Desagher, S., Holzer, M., Andrieux, A., Moutin, M.J., Janke, C., 2010. A family of protein-deglutamylating enzymes associated with neurodegeneration. Cell 143, 564–578.
Ronquist, F., Teslenko, M., van der Mark, P., Ayres, D.L., Darling, A., Hohna, S., Larget, B., Liu, L., Suchard, M.A., Huelsenbeck, J.P., 2012. MrBayes 3.2: efficient Bayesian phylogenetic inference and model choice across a large model space. Syst. Biol. 61, 539–542.
Salentin, S., Schreiber, S., Haupt, V.J., Adasme, M.F., Schroeder, M., 2015. PLIP: fully automated protein-ligand interaction profiler. Nucleic Acids Res. 43, W443–W447.
Santos, T.A.C., Silva, K.P., Souza, G.B., Alves, P.B., Menna-Barreto, R.F.S., Scher, R., Fernandes, R.P.M., 2023. Chalcone derivative induces flagellar disruption and autophagic phenotype in *Phytomonas serpens in vitro*. Pathogens 12, 423.
Saunders, E.C., Sernee, M.F., Ralton, J.E., McConville, M.J., 2021. Metabolic stringent response in intracellular stages of *Leishmania*. Curr. Opin. Microbiol. 63, 126–132.
Schmid-Hempel, P., Aebi, M., Barribeau, S., Kitajima, T., du Plessis, L., Schmid-Hempel, R., Zoller, S., 2018. The genomes of *Crithidia bombi* and *C. expoeki*, common parasites of bumblebees. PLoS One 13, e0189738.
Schneider, C.A., Rasband, W.S., Eliceiri, K.W., 2012. NIH image to ImageJ: 25 years of image analysis. Nat. Methods 9, 671–675.
Schwarz, R.S., Bauchan, G.R., Murphy, C.A., Ravoet, J., de Graaf, D.C., Evans, J.D., 2015. Characterization of two species of Trypanosomatidae from the honey bee *Apis mellifera*: *Crithidia mellificae* Langridge and McGhee, and *Lotmaria passim* n. gen., n. sp. J. Eukaryot. Microbiol. 62, 567–583.
Shang, Y., Li, B., Gorovsky, M.A., 2002. *Tetrahymena thermophila* contains a conventional gamma-tubulin that is differentially required for the maintenance of different microtubule-organizing centers. J. Cell Biol. 158, 1195–1206.
Shanmugasundram, A., Starns, D., Böhme, U., Amos, B., Wilkinson, P.A., Harb, O.S., Warrenfeltz, S., Kissinger, J.C., McDowell, M.A., Roos, D.S., Crouch, K., Jones, A.R., 2023. TriTrypDB: an integrated functional genomics resource for kinetoplastida. PLoS Negl. Trop. Dis. 17, e0011058.
Strobl, V., Yañez, O., Straub, L., Albrecht, M., Neumann, P., 2019. Trypanosomatid parasites infecting managed honeybees and wild solitary bees. Int. J. Parasitol. 49, 605–613.
Stuart, K., Brun, R., Croft, S., Fairlamb, A., Gürtler, R.E., McKerrow, J., Reed, S., Tarleton, R., 2008. Kinetoplastids: related protozoan pathogens, different diseases. J. Clin. Invest. 118, 1301–1310.
Sunter, J.D., Dean, S., Wheeler, R.J., 2023. TrypTag.org: from images to discoveries using genome-wide protein localisation in *Trypanosoma brucei*. Trends Parasitol. 39, 328–331.
Tiritelli, R., Cilia, G., Gómez-Moracho, T., 2025. The trypanosomatid (Kinetoplastida: Trypanosomatidae) parasites in bees: a review on their environmental circulation, impacts and implications. Curr. Res. Insect Sci. 7, 100106.

Vincent, I.M., Creek, D.J., Burgess, K., Woods, D.J., Burchmore, R.J., Barrett, M.P., 2012. Untargeted metabolomics reveals a lack of synergy between nifurtimox and eflornithine against *Trypanosoma brucei*. PLoS Negl. Trop. Dis. 6, e1618.

Votýpka, J., Klepetková, H., Yurchenko, V.Y., Horák, A., Lukeš, J., Maslov, D.A., 2012. Cosmopolitan distribution of a trypanosomatid *Leptomonas pyrrhocoris*. Protist 163, 616–631.

Votýpka, J., Kostygov, A.Y., Kraeva, N., Grybchuk-Ieremenko, A., Tesařová, M., Grybchuk, D., Lukeš, J., Yurchenko, V., 2014. *Kentomonas* gen. n., a new genus of endosymbiont-containing trypanosomatids of Strigomonadinae subfam. n. Protist 165, 825–838.

Wheeler, R.J., Gluenz, E., Gull, K., 2011. The cell cycle of *Leishmania*: morphogenetic events and their implications for parasite biology. Mol. Microbiol. 79, 647–662.

Wiśniewski, J.R., 2018. Filter-aided sample preparation for proteome analysis. Methods Mol. Biol. 1841, 3–10.

Yuan, X., Sun, J., Kadowaki, T., 2024. Aspartyl protease in the secretome of honey bee trypanosomatid parasite contributes to infection of bees. Parasit. Vectors 17, 60.

Yurchenko, V., Lukeš, J., Tesařová, M., Jirků, M., Maslov, D.A., 2008. Morphological discordance of the new trypanosomatid species phylogenetically associated with the genus *Crithidia*. Protist 159, 99–114.

Yurchenko, V., Votýpka, J., Tesařová, M., Klepetková, H., Kraeva, N., Jirků, M., Lukeš, J., 2014. Ultrastructure and molecular phylogeny of four new species of monoxenous trypanosomatids from flies (Diptera: Brachycera) with redefinition of the genus *Wallaceina*. Folia Parasitol. 61, 97–112.